

# Design of a dynamically configurable OADM device

Cuixia Dai<sup>1</sup>, Qianmin Dong<sup>2\*</sup>, Liren Liu<sup>3</sup>, Dean Liu<sup>3</sup>

1. Shanghai Institute of Technology, Shanghai, 200235. China

2. China Jiliang University, College of Information Engineering, 310018. China

3. Shanghai Institute of Optics and Fine Mechanics, Chinese Academy of Sciences, Shanghai, 201800. China

## ABSTRACT

A dynamically configurable optical add/drop multiplexer (OADM) device was proposed based on volume holographic gratings in doubly doped lithium niobate crystals and the principles of optical crystallography. The device consists of a wavelength demultiplexer module and an array of 2×2 electro-optic switches based on the internal reflection on the surface of the crystal. Two design schemes were presented: OADM based on discrete crystals with unifunctional integration and OADM based on monolithic crystal with multifunctional integration. This device can dynamically select signal channels that need to be added or dropped and simultaneously add/drop arbitrary signal channels. The suggested OADM has superior properties of simple and compact construction, convenient manipulation, lowered insertion losses and resistance to environmental perturbation.

**Keywords:** optical add/drop multiplexer (OADM), demultiplexer (DMUX) and electrooptical switching (EOSWA)

## 1. INTRODUCTION

With high development of the mobile communication and the internet application, the transmission capacity of the fiber-based circuitry increases fast. Since further bitrate increasing is limited by the electronic components in network, in recent years, more and more people prefer to using optical components to hold the optical characters of the signals, and a high demand for constructing an optical-based network is brought forward. Next generation of the optical-based internet communications requires new-style optical equipments to realize the real-time wavelength-division-multiplexing (WDM) channel processing. In our study, volume holographic gratings recorded in photorefractive crystals provide such a befitting technique.

In photorefractive material, multi-volume gratings can be recorded in a crystal, and thus the angle multiplexing and the wavelength multiplexing can be performed[1-4]. By combining the holographic-multiplexing-volume-grating with a certain WDM channel, merits of the high selectivity of Bragg wavelength and reading angle of the volume hologram can be utilized in the optical communication system. In our study, dual-wavelength method is used[5-9]. by using the visible light which the crystal is sensitive to to record grating, and using the infrared light which is usually used in optical communication to read the grating, the volume grating is recorded and fixed, and will not be destroyed for the long-time reading. Moreover, two-center LiNbO<sub>3</sub>:Ce:Cu crystals are also used in our system. In these crystals, gratings are simultaneously recorded in shallow and deeper centers and finally fixed in the deeper center, which realizes the nonvolatile holographic recording[10-12]. Furthermore, LiNbO<sub>3</sub> crystals hold such physical characters as electro-optical

---

\* [qmdong@cjlu.edu.cn](mailto:qmdong@cjlu.edu.cn)

effect, piezoelectricity and calorescence, etc. So we can use these characters in a multifunctional integration to construct a optical communication system.

In this paper, an OADM device was proposed based on volume holographic gratings in  $\text{LiNbO}_3\text{:Ce:Cu}$  crystals and the principles of optical crystallography. The dual-wavelength method of nonvolatile recording is discussed, the basic principle of this device is presented, the scheme of this design and the optimization method are given, and the performance process of this device is described.

## 2. NONVOLATILE RECORDING IN $\text{LiNbO}_3\text{:CE:CU}$ CRYSTAL

In general, two processing phases are necessary in nonvolatile recording in two center  $\text{LiNbO}_3$  crystals with dual-wavelength. In the first recording phase, the crystal is illuminated simultaneously with two visible beams for interference recording, the recording space-charge field (SCF) gratings are created both in the shallow traps and the deep traps. In the second optical fixing phase, only near-infrared beam is used to read, the SCF grating in the shallow traps may be somewhat erased, but the SCF grating in the deep traps could be always remained, thus building up a nonvolatile system. The two-center holographic recording can be described by Kukhtarev equations modified for doubly doped crystals. The material equations [10-12] can be separated into two sets of zeroth and first-order equations as follows

$$\frac{\partial N_{D0}^-}{\partial t} = -g_D N_{D0}^- + \gamma_D N_{e0} (N_D - N_{D0}^-) \quad (1)$$

$$\frac{\partial N_{S0}^-}{\partial t} = -g_S N_{S0}^- + \gamma_S N_{e0} (N_S - N_{S0}^-) \quad (2)$$

$$N_{e0} = \frac{g_D N_{D0}^- + g_S N_{S0}^-}{\gamma_D (N_D - N_{D0}^-) + \gamma_S (N_S - N_{S0}^-)} \quad (3)$$

And

$$\frac{\partial N_{D1}^-}{\partial t} = -g_D N_{D1}^- - S_{D,L} m I_{L0} N_{D0}^- + \gamma_D N_{e1} (N_D - N_{D0}^-) - \gamma_D N_{e0} N_{D1}^- \quad (4)$$

$$\frac{\partial N_{S1}^-}{\partial t} = -g_S N_{S1}^- - S_{S,L} m I_{L0} N_{S0}^- + \gamma_S N_{e1} (N_S - N_{S0}^-) - \gamma_S N_{e0} N_{S1}^- \quad (5)$$

$$N_{e1} = \frac{\left\{ (g_D + \gamma_D N_{e0}) N_{D1}^- + (g_S + \gamma_S N_{e0}) N_{S1}^- - \frac{e\mu N_{e0}}{\varepsilon \varepsilon_0} (N_{D1}^- + N_{S1}^-) - \frac{iK}{e} [\kappa_D N_{D1}^-] \right.}{\left. + \kappa_S N_{S1}^- + (\kappa_{D,L} N_{D0}^- + \kappa_{S,L} N_{S0}^-) m I_{L0} \right\} + (S_{D,L} N_{D0}^- + S_{S,L} N_{S0}^-) m I_{L0}} \quad (6)$$

$$\gamma_D (N_D - N_{D0}^-) + \gamma_S (N_S - N_{S0}^-) + \frac{e\mu N_{e0}}{\varepsilon \varepsilon_0} + \frac{K_B T \mu K^2}{e}$$

Where  $g_D = S_{D,L} I_{L0} + S_{D,H} I_H$  ,  $g_S = S_{S,L} I_{L0} + S_{S,H} I_H$  ,  $\kappa_D = \kappa_{D,L} I_{L0} + \kappa_{D,H} I_H$  ,  $\kappa_S = \kappa_{S,L} I_{L0} + \kappa_{S,H} I_H$  ;

The subscripts  $D$  and  $S$  indicate the deep and shallow centers, and  $L$  and  $H$  indicate the lower and higher frequency light, respectively;  $N$ ,  $N^-$ , and  $N_e$  are the densities of centers, the electron in centers, and the conducting electron, respectively;  $\gamma$ ,  $S$ ,  $\kappa$ ,  $T$ ,  $K_B$ ,  $I$ ,  $m$  and  $K$  are the recombination coefficient, the photo-excitation constant, the bulk photovoltaic coefficient, crystal temperature, Boltzmann constant, the intensity of light, the modulation depth of recording light and the spatial frequency of interference pattern, respectively;  $\varepsilon_0$ ,  $e$ ,  $\varepsilon$  and  $\mu$  are the permittivity of free space, the electron charge, the dielectric coefficient and the electron mobility in the conduction band, respectively.

The space-charge field (SCF)  $E_{sc}$  can be expressed

$$E_{sc} = \frac{-ie}{\epsilon\epsilon_0 K} (N_{D1}^- + N_{S1}^- + N_{e1}) \quad (7)$$

The depth of the refractive-index change (RIC)  $n_1$  and the SCF  $E_{sc}$  are related by the linear electro-optic effect

$$n_1 = \frac{n_o^3 \gamma_{eff} |E_{sc}|}{2} \quad (8)$$

Where  $n_o$  is the average refractive-index of LiNbO<sub>3</sub> crystal to the recording light and  $\gamma_{eff}$  is the effective electro-optic coefficient.

The vectorgraph of the volume grating recorded by visible light and read by near-infrared light is shown in Fig.1(a). Where,  $\mathbf{K}_w^i$  and  $\mathbf{k}_w^d$  are wave vectors of the sample light and the reference light, respectively.  $\theta_1$  and  $\theta_2$  are the incident angles of the sample light and reference light to the normal of the crystal surface, respectively.  $\mathbf{K}_r^i$  and  $\mathbf{k}_r^d$  are wave vectors of the reading light and the diffracted light, respectively. And  $\phi_1$  and  $\phi_2$  are angles of tilt of the reading light and the diffracted light, respectively. The wavelength of recording light and reading light can be written as  $\lambda_w$  and  $\lambda_r$  respectively.  $\mathbf{K}$  is the vector of grating, and the  $\Lambda$  is the grating spacing which is determined by the recording configuration and the wavelength.

$$\Lambda = \frac{\lambda_w}{2 \sin(\frac{\theta_1 + \theta_2}{2})} = \frac{2\pi}{K} \quad (9)$$

Where,  $K$  is the value of  $\mathbf{K}$ .

According to the diffraction theory, the recording light and the reading light should obey the bragg 's law to obtain the maximum of diffracted light.

$$\frac{\lambda_w}{\sin(\frac{\theta_1 + \theta_2}{2})} = \frac{\lambda_r}{\sin(\frac{\phi_1 + \phi_2}{2})} \quad (10)$$

Where,  $\theta_1 - \theta_2 = \phi_1 - \phi_2$

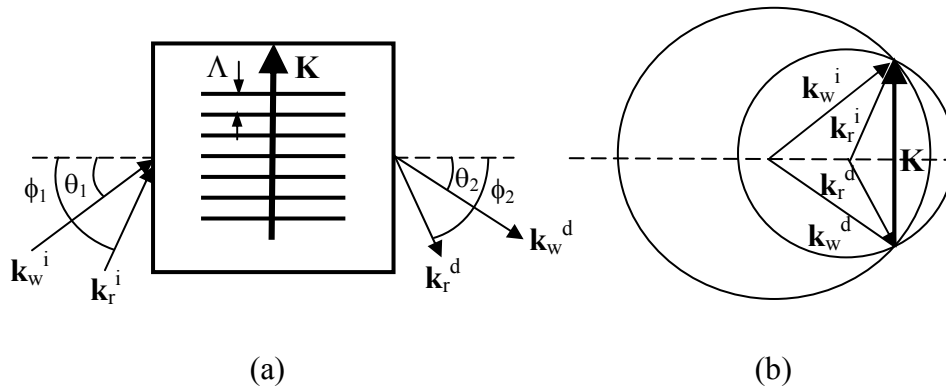


Fig.1 (a) vectorgraph of  $\mathbf{K}$  and (b) circle vector diagram of  $\mathbf{K}$  in a grating recorded with visible light and read with near infrared light.

In principle, if the grating spacing and the wavelength of reading light are determined, the incident angle of the reading light should be exclusively determined. vice versa, if the grating spacing and reading angle are determined, the wavelength of reading light should be determined. Particularly, when the grating is recorded with a symmetrical configuration( $\theta_1=\theta_2$ ), and read with a vertical configuration, angle between the read light and the diffracted light in the crystal should be  $90^\circ$ . Then the Bragg' law can be amended to be as follows:

$$\lambda_w = \sin \theta_1 \frac{\lambda_r}{\sqrt{2}n_o} \quad (11)$$

Where,  $n_o$  is the the refractive index of the crystal for the ordinary -polarized reading wavelength  $\lambda_r$ .

Fig. 1(b) gives the circle vector diagram of  $\mathbf{K}$  in a grating recorded with visible light and read with near infracted light. It can be seen obviously that vectors of incident light  $\mathbf{k}_{w,r}^i$ , of the diffracted light  $\mathbf{k}_{w,r}^d$  and the grating vector  $\mathbf{K}$  should obey Bragg's law :

$$\mathbf{K} = \mathbf{k}_w^i - \mathbf{k}_w^d = \mathbf{k}_r^i - \mathbf{k}_r^d \quad (12)$$

### 3. SCHEME OF OADM DESIGN AND THE OPTIMIZATION METHOD

#### 3.1 scheme of OADM based on discrete crystals with unifunctional integration

The OADM device is set up based on volume holographic gratings in doubly doped lithium niobate crystals and the principles of optical crystallography. Performence of the system can be made by integrating several functional unites in  $\text{LiNbO}_3$  crystal, such as the demultiplexer (DMUX) and the electrooptical switching array (EOSWA). As shown in Fig.2, scheme of the OADM design is made up of several pieces of  $\text{LiNbO}_3$  crystals is given. There are two functional unites in this system: DMUX and EOSWA. DMUX is composed of four volume holographic gratings ( $\text{HG}_1\text{-HD}_4$ ) in four doubly doped lithium niobate crystals separately, and it will perform demultiplex the for WDM multi-wavelength signals. The crystal is monocrystal of the  $\text{LiNbO}_3$  which have been grown in the air by the Czochralski method and annealed at  $900^\circ\text{C}$  in air for 6 hours and then cooled down to room temperature. The crystals are cut to  $5\text{ mm}\times 5\text{ mm}\times 30\text{ mm}$  and all sides are polished to optical quantity. Four volume holographic gratings are arranged uniformly-spaced along the direction parallel to the long edge of the crystal, and the distance between them is 6mm.

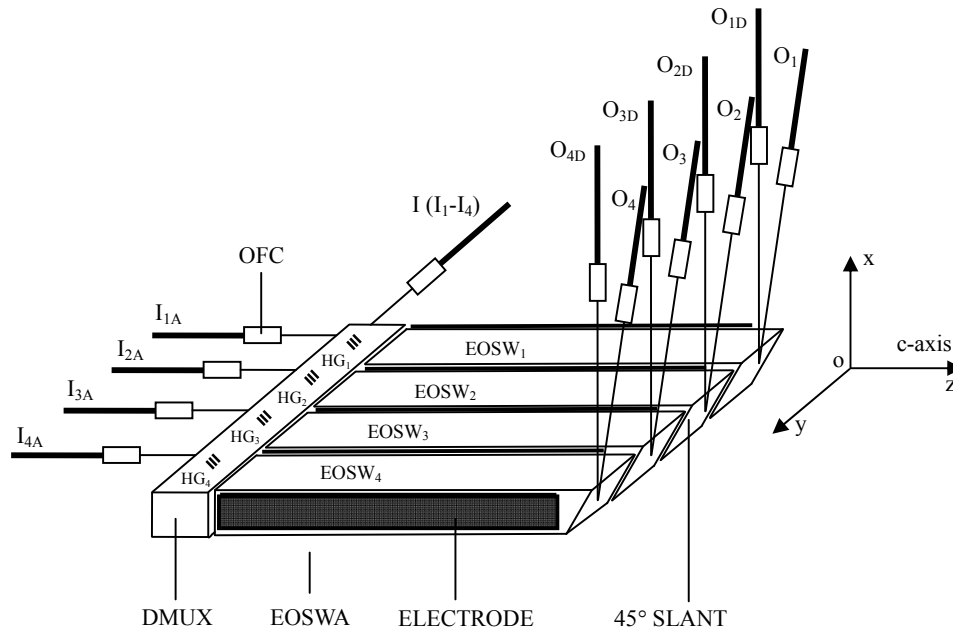


Fig.2 scheme of OADM design using discrete crystals with unfunctional integration.

EOSWA is composed of four  $2 \times 2$  EOSWs (EOSW<sub>1</sub>-EOSW<sub>4</sub>) which have the same configuration. The internal reflecting  $2 \times 2$  EOSW is made with a single LiNbO<sub>3</sub> crystal and Cu electrodes are attached to both sides of it (see "ELECTRODE" part in Fig.2). The crystal is processed to be a  $45^\circ$  slant hexahedron and the length of upper and lower surface of it are 45 mm and 40 mm, respectively, the width and the depth are both 5mm. All sides of the crystal are polished to optical quantity. The size of electrode is  $40 \times 4 \times 1$  mm<sup>3</sup>, and it is connected with direct-current-high-voltage power supply which will add half-wave voltage transverse to the crystal to change the polarization of signals.

In the OADM system, WDM signal I have four wavelength channels I<sub>1</sub>-I<sub>4</sub>. The wavelength of signal I<sub>i</sub> ( $i=1,2,3,4$ ) is  $\lambda_i$ , and the vibrant direction of the electrical vector is parallel to x direction. I<sub>1A</sub>-I<sub>4A</sub> are four local add input signals, the wavelength of I<sub>iA</sub> ( $i=1,2,3,4$ ) is  $\lambda_i$ , and the vibrant direction of the electrical vector is parallel to y direction. O<sub>1</sub>-O<sub>4</sub> are four line output signal, and O<sub>1D</sub>-O<sub>4D</sub> are the local drop output signals, the wavelengths of signal O<sub>i</sub> and O<sub>iD</sub> ( $i=1,2,3,4$ ) are all  $\lambda_i$ , and the vibrant directions are vertical to each other. The fiber collimator (OFC) can coupled signals from fiber to crystal or from crystal to fiber.

With DMUXs and EOSWAs, the OADM can realize four wavelength add /drop multiplexing. The working principle of this system can be described as follows: by demultiplexing signals I with DMUX, each mono-wavelength signal I<sub>i</sub> ( $i=1,2,3,4$ ) transfers to their EOSW<sub>i</sub> ( $i=1,2,3,4$ ). Simultaneously, each local add input mono-wavelength signal I<sub>iA</sub> ( $i=1,2,3,4$ ) transfers in EOSW<sub>i</sub> ( $i=1,2,3,4$ ). By controlling states of the EOSWs, the wavelength channel of add/drop can be dynamically selected, and each arbitrary signal channel or multi-signal channels can be simultaneously achieved. The equipment can realize the dynamical reconstruction, and the number of wavelength division multiplexing signal channel can be expanded to 8 and 16 just by increasing volume holographic gratings to a corresponding number. This scheme has superior properties of simple construction, convenient manipulation, lowered insertion losses and resistance to environmental perturbation, and there will be a promising application for it.

Working principle of DMUX and EOSW made in  $\text{LiNbO}_3\text{:Ce:Cu}$  crystals can be seen in Fig.3(a) and Fig.3(b), respectively. By recording volume holographic gratings in advance with proper angel interval in  $\text{LiNbO}_3\text{:Ce:Cu}$  crystals, the function of DMUX can be realized. Different wavelengths just can be diffracted by different gratings with Bragg' angle matching, and they will transmit along different directions. So different wavelength can be divided after the DMUX. Fig.3(a) gives the working principle of the DMUX in a vertically reading configuration. Fig. 3(b) shows the working principle of the total internal reflection  $2\times 2$  EOSW. By using the transverse electro-optic effect in  $\text{LiNbO}_3\text{:Ce:Cu}$  crystals, the polarization of signals can be controled. Two orthogonal polarizations of ordinary and extraordinary light can be divided.

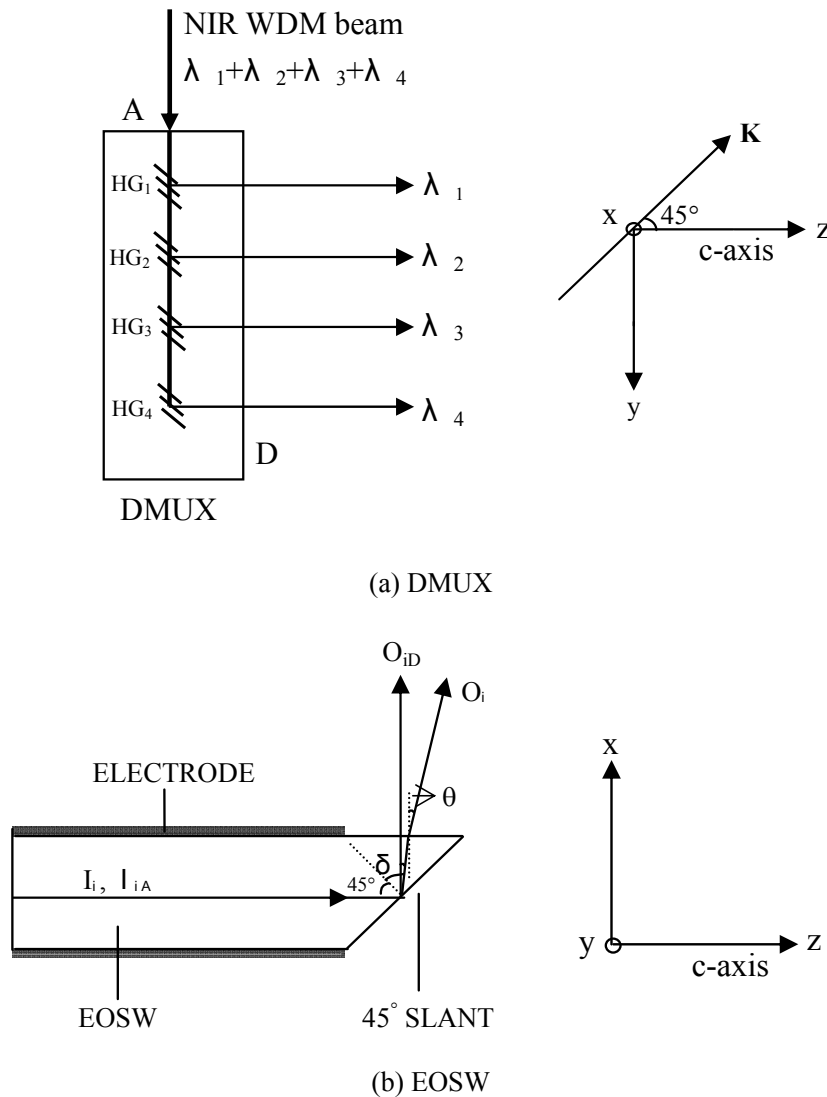


Fig.3 working principle of (a) DMUX and (b) EOSW

### 3.2 OADM based on monolithic crystal with multifunctional integration

In the above scheme, one piece of crystal can just act as a unifunctional unite, and thus decreasing the use efficiency. And using discrete components will surely add insertion losses, and the system will more sensitive to environmental

perturbation. Because the number of channels in this system is limited by the number of the crystals, efforts should be done for more than cost saving. In our study, OADM based on monolithic crystal with multifunctional integration is proposed.

As shown in Fig.4, the DMUX and the EOSWA are integrated into a single  $\text{LiNbO}_3\text{:Ce:Cu}$  crystal. The crystal is processed into a  $45^\circ$  slant cuboid and cut into  $50 \times 30 \times 5 \text{ mm}^3$ . All sides of the crystal are polished to optical quantity and the optical axis of it is along the  $z$  direction. The size of DMUX is  $5 \times 30 \times 5 \text{ mm}^3$ , and volume gratings recorded in advance are arranged uniformly-spaced along  $y$  direction with the distance  $7.5 \text{ mm}$  between them. The size of EOSWA is  $45 \times 30 \times 5 \text{ mm}^3$ , and it is made up of four  $40 \times 4 \text{ mm}^2$  electrodes which are evaporated onto the upper and lower surfaces of the crystal and arranged uniformly-spaced alignment to the corresponding volume gratings along  $y$  direction.

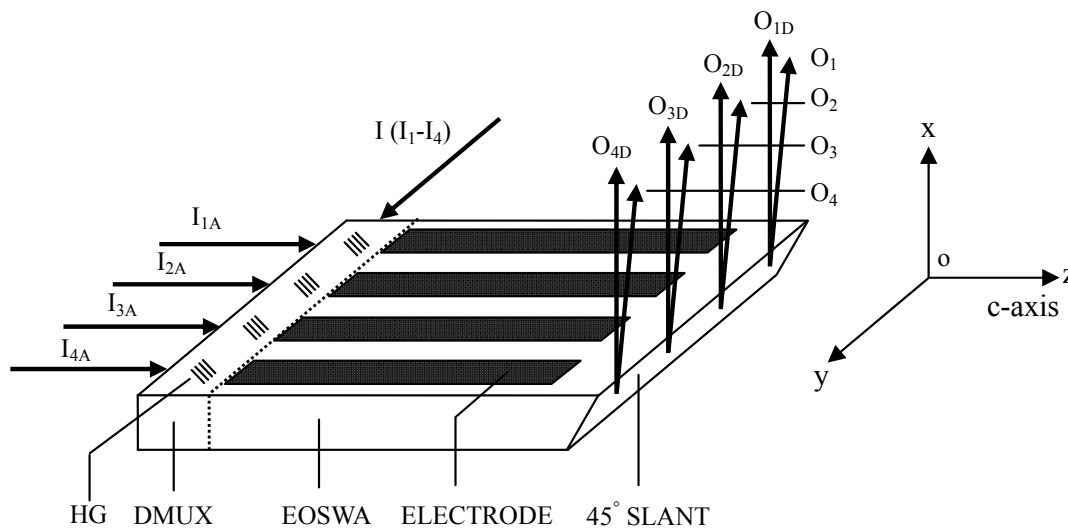


Fig.4. Scheme of OADM design using monolithic crystal with multifunctional integration

The OADM system constructed with monolithic crystal is an optimized design based on  $\text{LiNbO}_3\text{:Ce:Cu}$ . The working principle is as that using discrete crystals with unfunctional integration. But the configuration is much simple and much compact, the use efficiency is highly increased, and it is convenient for miniaturization and intergration. Since the whole system is just made up of a monolithic  $\text{LiNbO}_3\text{:Ce:Cu}$  crystal, no component can be moved, it has superior property of high resistance to environment such as heat, electromagnetic field and vibration. It can be performed stably and reliably. The device has other superior properties of low cost and easy for assemblage, so it is suit for mass manufacturing.

#### 4. CONCLUSIONS

In this paper, an OADM system is proposed based on volume holographic gratings in  $\text{LiNbO}_3\text{:Ce:Cu}$  crystal. Two basic functional components are involved: DMUX based on volume holographic grating and EOSW based on the principles of optical crystallography. Using the Bragg' selectivity of volume holographic grating, demultiplexing can be realized for WDM signals. Using linear electro-optic effect,  $2 \times 2$  EOSWs can be achieved. Two design schemes are presented:

OADM based on discrete crystals with unfunctional integration and OADM based on monolithic crystal with multifunctional integration. This device can dynamically select signal channels that need to be added or dropped and simultaneously add/drop arbitrary signal channels. The suggested OADM has superior properties of simple and

compact construction, convenient manipulation, lowered insertion losses and resistance to environmental perturbation.

## ACKNOWLEDGEMENTS

The authors gratefully acknowledge the support of China Postdoctoral Science Foundation Funded Project (project number: 20070410714), the support of Science and Technology Commission of Shanghai Municipality Funded Project (project number: 09ZR1431300), the support of Shanghai Education Committee Funded Project on Scientific Research for Outstanding Young Teacher, and the support of Shanghai Institute of Technology Funded Project for Newly Entering Young Teacher .

## REFERENCES

- [1]. Mok F. H., "Angle-multiplexed storage of 5000 holograms in  $\text{LiNbO}_3$ ," *Opt. Lett* 16(12), 915-917 (1993).
- [2]. Lee M., Takekawa S., Furukawa Y., Kitamura K., Hatano H., Tao S., "Angle-multiplexed hologram storage in  $\text{LiNbO}_3\text{:Tb:Fe}$ ," *Opt. Lett* 25(18), 1337-1339(2000) .
- [3]. F. T. S. Yu, S.Wu, A. W. Mayers, S. Rayan, "Wavelength-multiplexed reflection matched spatial filters using  $\text{LiNbO}_3$ ," *Opt. Commun.* 81 (6), 343–347(1991) .
- [4]. Adibi A, Buse K, Psaltis D., "Hologram multiplexing using two-step recording," *Proc. SPIE* 3468, 20-29 (1998).
- [5]. Buse K., Jermann F., Kratzig E., "Two-step photorefractive hologram recording in  $\text{LiNbO}_3\text{:Fe}$ ," *Ferroelectrics* 141(2), 197-205(1993).
- [6]. Buse K, Adibi A, Psaltis D., "A novel method for persistent holographic recording in doubly-doped lithium niobate," *Proc. SPIE* 3638, 15-21(1999) .
- [7]. X. Zhang, J. Xu, Q. Sun, S. Liu, G. Zhang, Dual-wavelength nonvolatile holographic storage, *Opt. Commun.*, 2000, 180, 211-215.
- [8]. Buse K., Jermann F., Kratzig E., "Infrared holographic recording in  $\text{LiNbO}_3\text{:Cu}$ ," *Appl. Phys. A*.58(3), 191-195(1994).
- [9]. Buse K., Jermann F., Kratzig E., "Infrared holographic recording in  $\text{LiNbO}_3\text{:Fe}$  and  $\text{LiNbO}_3\text{:Cu}$ ," *Opt. Mater*4(2-3), 237-240(1995).
- [10]. Liu Y., Liu L., Zhou C., Xu L., "Photorefractive holographic dynamics in doubly doped  $\text{LiNbO}_3\text{:Fe:Mn}$ ," *Chin. Phys. Lett*17(8), 571-573(2000).
- [11]. D. Psaltis, F. Mok, H. S. Li, "Nonvolatile storage in photorefractive crystals, " *Opt. Lett* 19(8), 210-212(1994).
- [12]. Buse K, Adibi A, Psaltis D., "Efficient non-volatile holographic recording in doubly-doped lithium niobate," *J. Opt. A: pure Appl. Opt.* 1, 237-238(1999).